INTELLIGENT FUSION OF SATELLITE IMAGERY DATA

Michel Morgan
Woolpert Inc.
Dayton, OH
michel.morgan@woolpert.com

ABSTRACT

The number of satellites collecting imagery data has been increasing providing large amount of data at increasing resolution. It is a challenge to geometrically correct this mass data in a timely manner especially for real or near real time applications such as natural hazard monitoring/mitigation. Geo-referencing is to establish the relationship between images and the object space, and could be done directly or indirectly. In direct geo-referencing, a well calibrated sensor and very accurate GPS/IMU units are must have since any small errors in the sensor's interior or exterior orientation parameters are magnified and propagate as large errors in the object space. Alternatively, indirect geo-referencing utilizes control information to achieve the same goal. Traditional control information comes in the form of control points which are expensive to collect in the object space in addition to the inaccessibility of ground targets in many scenarios such as in military applications and hazardous environments. In this paper, a first order polynomial correction is introduced to the rational polynomial coefficients model in an attempt to increase the accuracy while reducing the requirement of control points.. Experimental results using IKONOS imagery over the city of Calgary are presented achieving sub-pixel accuracy.

Key words: Satellite imagery, rational polynomial coefficients (RPC), bias correction

INTRODUCTION

Satellite imagery provides great ground coverage at competitive cost. Advancement in technology facilitates reaching higher spatial, spectral resolution. Repetitive coverage allows for selection from several datasets and enables change detection. In addition, being captured through great extent of the atmosphere they possess valuable information not only for Earth's surface but also for the atmosphere. In general, satellite images are used for many applications including natural hazard mitigation, emergency response planning, homeland defense and security, port and border enforcement, land use planning and change detection, urban planning, natural resources, meteorology, agricultural and environmental applications, etc.

Advantages of satellite images can be hindered or undermined if high spatial accuracy is not reached. Several geometric models and approaches exist aiming at obtaining the best accuracy. Rigorous modeling is the most accurate approach since it takes into consideration the actual physical process of image capture. It requires both sensor's internal and external characteristics to be available. The former is usually available through a calibration process, while the later requires additional information regarding the sensor's exterior orientation which is usually available from GPS/IMU instruments. Both interior and exterior orientation parameters have to be of high accuracy which imposes more challenges to direct geo-referencing process, where no ground control information is used. Ground control however can increase the attained accuracy by correcting for sensor's interior and/or exterior orientation parameters in an indirect geo-referencing process.

It would be ideal if both sensor's interior and exterior orientation characteristics (in terms of physical description and not necessarily numerical values) are available with an abundance of ground control information. However, the interior and exterior orientation characteristics (rigorous model in short) are usually concealed from the user community. In addition control information in form of ground control points are expensive to acquire. Other replacement models exist. Among which are rational polynomial coefficients (RPC), direct linear transformation (DLT), self-calibrating direct linear transformation (SDLT), parallel projection, modified parallel projection, etc. (Morgan et al, 2006; Tao and Hu, 2001; Wang, 1999; Abdel-Aziz and Karara, 1971). From the user's perspective, these replacement models do not require the knowledge of either sensor's interior orientation parameters. However, these parameters are used by the satellite image provider in order to obtain some of these replacement models such as RPC (Tao and Hu, 2001). With the exception of RPC, all other replacement models require control points to start with. Only RPC could have been used right away for mapping if not for the biases exist in any or both of interior

and exterior orientation parameters. Therefore, ground control information is required to correct for these errors. The following section briefly describes RPC followed by the proposed approach to compensate for the errors in these coefficients. Experimental results are then presented followed by conclusions and recommendations for future work.

UTILIZING RATIONAL POLYNOMIAL COEFFICIENTS (RPC)

Mathematical Representation of RPC

Using RPC, a point whose object space coordinates are (X, Y, Z) relates to its image coordinates (r, c) as ratios of polynomials, as shown in Equation 1.

$$r = \frac{\sum_{n=1}^{20} A_n X^i Y^j Z^k}{\sum_{n=1}^{20} B_n X^i Y^j Z^k}$$
$$c = \frac{\sum_{n=1}^{20} C_n X^i Y^j Z^k}{\sum_{n=1}^{20} D_n X^i Y^j Z^k} \qquad \text{(Equation 1)}$$

for all $i+j+k \leq 3$, where, $A_1,\ldots,A_{20}$, $B_1,\ldots,B_{20}$, $C_1,\ldots,C_{20}$, $D_1,\ldots,D_{20}$ are the rational polynomial coefficients. These coefficients are determined by satellite imagery provider through post processing of the sensor's interior and exterior orientation parameters (Tao and Hu, 2001).

Refining RPC

As indicated by many researchers (Morgan et al, 2006; Wang, 1999; Okamoto at al, 1992), there is no real need for having extremely large number of parameters to achieve high geometric accuracy. Therefore, we introduce set of corrections to RPC as expressed in Equation 2.

$$r = \frac{\left(\sum_{n=1}^{20} A_n X^i Y^j Z^k\right) + \alpha_1 + \alpha_2 X + \alpha_3 Y + \alpha_4 Z}{\left(\sum_{n=1}^{20} B_n X^i Y^j Z^k\right) + \beta_2 X + \beta_3 Y + \beta_4 Z}$$
$$c = \frac{\left(\sum_{n=1}^{20} C_n X^i Y^j Z^k\right) + \gamma_1 + \gamma_2 X + \gamma_3 Y + \gamma_4 Z}{\left(\sum_{n=1}^{20} D_n X^i Y^j Z^k\right) + \delta_2 X + \delta_3 Y + \delta_4 Z} \qquad \text{(Equation 2)}$$

where $\alpha_1,\ldots, \alpha_4$, $\beta_2,\ldots, \beta_4$, $\gamma_1,\ldots, \gamma_4$, $\delta_2,\ldots, \delta_4$ are the corrections to RPC. The main reason behind introducing them in this way is to enable us to combine them with the original parameters to produce different set of RPC. For example, α_1 will be added to A_1, β_2 will be added to B_2, and so forth. In this case, the new corrections can be easily accounted for and final parameters will conform to RPC model to be easily used by different software packages that support RPC.

These set of additional parameters can be extended to include corrections to all original parameters. However, as mentioned earlier, previous research suggested that not many parameters are required for modeling satellite imagery. Therefore, we will be introducing only first order corrections. Furthermore, we will be investigating the reduction of these additional parameters to reach the optimal set of corrections that will significantly improve the accuracy without over-parameterization.

Photogrammetric Triangulation Using RPC

Aerial triangulation, or photogrammetric triangulation in general, is used to reduce the requirement of control points per image. For this purpose, several points are used in order to tie images together to form one entity (relative orientation) and control points are used to correctly geo-reference the block (absolute orientation). Thus, if there were a minimum requirement of control points per image, such a requirement is transferred to the entire block as a single entity and is not longer a requirement for each individual image. In addition, each control point does not need to be measured in all images where it appears (although additional redundancy is useful to detect blunders). Instead, it can be measured in only single image. These are the main motives behind developing a photogrammetric triangulation using RPC and utilizing both control and tie points. In this triangulation, the unknown parameters are:

- All or subset of the corrections ($\alpha_1,\ldots, \alpha_4, \beta_2,\ldots, \beta_4, \gamma_1,\ldots, \gamma_4, \delta_2,\ldots, \delta_4$)
- Object coordinates of tie points

Observation values include:

- Image coordinates of tie and control points
- Object coordinates of control points

while original RPC values are treated as constants. Different scenarios will be generated based on different sets of correction parameters as shown in Table 1.

Table 1. Different Scenarios for Different Sets of Correction Parameters.

Scenario	Unknown Parameters	Notes
I	α_1, γ_1	Shift
II	$\alpha_2, \alpha_3, \gamma_2, \gamma_3$	Rotation, non-orthogonally, two scales
III	α_4, γ_4	Height
IV	$\alpha_1, \alpha_2, \alpha_3, \gamma_1, \gamma_2, \gamma_3$	Standard Affine
V	$\alpha_1, \alpha_4, \gamma_1, \gamma_4$	Shift, Height
VI	$\alpha_1, \alpha_2, \alpha_3, \alpha_4, \gamma_1, \gamma_2, \gamma_3, \gamma_4$	2D Affine (Parallel Projection)
VII	$\alpha_1, \alpha_2, \alpha_3, \beta_2, \beta_3, \gamma_1, \gamma_2, \gamma_3, \delta_2, \delta_3$	Projective
VIII	$\alpha_1, \alpha_2, \alpha_3, \alpha_4, \beta_2, \beta_3, \beta_4, \gamma_1, \gamma_2, \gamma_3, \gamma_4, \delta_2, \delta_3, \delta_4$	DLT

EXPERIMENTAL RESULTS

The main objectives of the experiments in this section are to:

- Determine the best combinations out of those listed in Table 1 that achieve the highest accuracy.
- Determine the minimum number of control points required to achieve this accuracy

A set of three IKONOS imagery (of 1 meter nominal resolution) over the city of Calgary together with provided RPC values were used in the experiments. A total of 13 control points were collected, see Figure 1. Some of these points were used as control while others used as tie and check points.

We start the experiments by assessing the quality of provided RPC. We performed a forward intersection using the image coordinates of 13 check points (Experiment 1, Table 2). By comparing them with the known values, one can see large amount in bias in all directions as shown in the same table. In Experiments 2 to 9, nine control points were used, with all possible scenarios from Table 1, and the results are listed in Table 2. From this table, Experiments 3 and 4 show large error values. No shift values were introduced in Scenarios II & III, thus we can conclude that shifts in both direction are among most important corrections to account for. By comparing the results of Experiments 2, 5 to 9, one cannot see a significant improvement, although Experiment 9 is slightly better than the rest. In these experiments, nine control points were used. In the next set of experiments, we would to examine the performance of these models while reducing the number of control points in order to find the minimum control requirement. Scenarios I (shift), IV (standard Affine), VI (2D Affine), VII (projective) and VIII (DLT) were selected to carry on the next set of experiments, Tables, 3 to 7.

From these experiments, one can immediately see the deterioration of the performance of these models as the number control points is reduced. However, for the majority of these models (with the exception of Scenario VIII that corresponds to DLT), five control points result in sub-pixel accuracy. Although DLT slightly outperformed other models using nine control points, it did not perform very well using fewer control points. This comes at no surprise since more parameters are needed for DLT compared to other models.

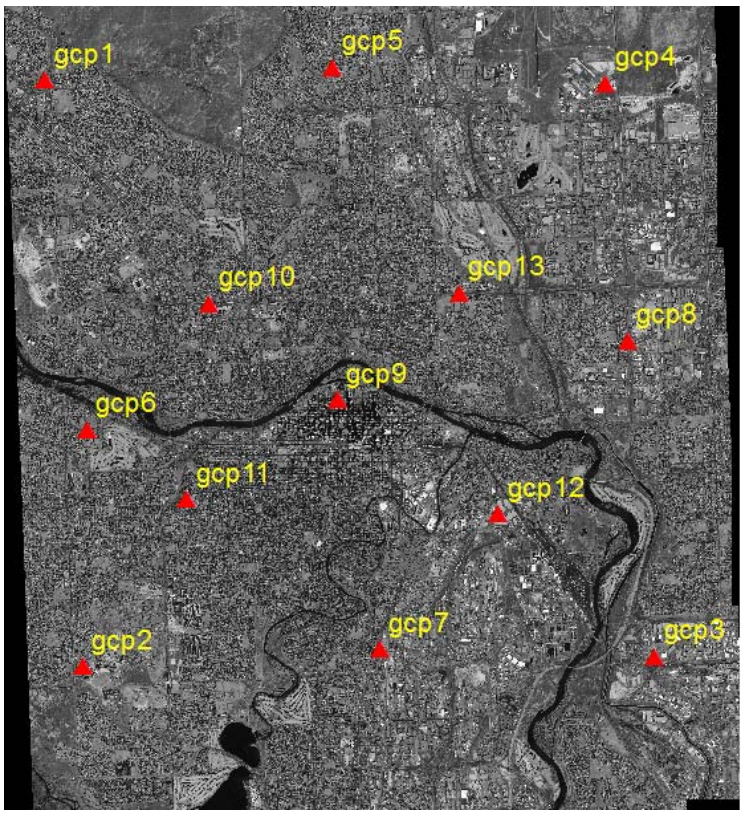

Figure 1. IKONOS Imagery over the City of Calgary and 13 Ground Control Points.

Table 2. Errors Computed at Checkpoints for Different Correction Models.

Experiment #	Scenario	Number of Control Points	Estimation	Errors at checkpoints (Mean ± Std), meters			
				X	Y	Z	Spatial Error
1	-	0	Forward intersection	-13.11±0.41	-3.86±0.57	-22.36±0.81	26.21±1.07
2	I	9	Bundle Adjustment	-0.03±0.45	0.02±0.59	-0.38±0.37	0.38±0.83
3	II	9	Bundle Adjustment	-2.76±0.40	2.15±0.52	8.68±0.30	9.36±0.72
4	III	9	Bundle Adjustment	-2.77±0.97	2.20±0.85	8.20±1.95	8.93±2.34
5	IV	9	Bundle Adjustment	-0.05±0.33	0.03±0.38	-0.50±0.53	0.50±0.73
6	V	9	Bundle Adjustment	-0.04±0.44	-0.11±0.39	-0.48±0.50	0.49±0.77
7	VI	9	Bundle Adjustment	-0.12±0.33	-0.03±0.37	-0.44±0.49	0.46±0.70
8	VII	9	Bundle Adjustment	-0.01±0.32	0.07±0.38	-0.32±0.55	0.33±0.74
9	VIII	9	Bundle Adjustment	-0.04±0.30	0.07±0.29	-0.28±0.55	0.29±0.69

Table 3. Error Computed at Checkpoints by Varying the Number of Control Points for Scenario I (Shift).

Experiment #	Scenario	Number of Control Points	Estimation	Errors at checkpoints (Mean ± Std), meters			
				X	Y	Z	Spatial Error
10	I	1	Bundle Adjustment	-0.85±0.34	-0.07±0.66	1.11±0.89	1.40±1.16
11	I	2	Bundle Adjustment	0.25±0.38	-0.59±0.52	-0.58±0.86	0.86±1.07
12	I	3	Bundle Adjustment	-0.15±0.46	0.26±0.71	-0.73±0.79	0.79±1.16
13	I	4	Bundle Adjustment	0.21±0.41	-0.05±0.49	-0.43±0.82	0.48±1.04
14	I	5	Bundle Adjustment	-0.07±0.33	-0.06±0.53	-0.07±0.82	0.12±1.03
15	I	8	Bundle Adjustment	0.23±0.52	0.03±0.51	-0.66±0.45	0.70±0.86
16	I	9	Bundle Adjustment	-0.03±0.44	0.02±0.59	-0.38±0.37	0.38±0.82

Table 4. Error Computed at Checkpoints by Varying the Number of Control Points for Scenario IV (Affine).

Experiment #	Scenario	Number of Control Points	Estimation	Errors at checkpoints (Mean ± Std), meters			
				X	Y	Z	Spatial Error
17	IV	1	Bundle Adjustment	-	-	-	-
18	IV	2	Bundle Adjustment	-0.22±4.20	0.49±0.70	1.09±16.64	1.22±17.18
19	IV	3	Bundle Adjustment	0.41±0.32	-0.59±0.66	-0.88±0.57	1.13±0.93
20	IV	4	Bundle Adjustment	0.20±0.38	-0.04±0.51	-0.55±0.62	0.59±0.89
21	IV	5	Bundle Adjustment	-0.07±0.30	-0.07±0.55	-0.15±0.57	0.18±0.84
22	IV	8	Bundle Adjustment	0.21±0.46	0.06±0.33	-0.79±0.55	0.82±0.79
23	IV	9	Bundle Adjustment	-0.05±0.33	0.03±0.38	-0.50±0.53	0.51±0.73

Table 5. Error Computed at Checkpoints by Varying the Number of Control Points for Scenario VI (2D Affine).

Experiment #	Scenario	Number of Control Points	Estimation	Errors at checkpoints (Mean ± Std), meters			
				X	Y	Z	Spatial Error
24	VI	1	Bundle Adjustment	-	-	-	-
25	VI	2	Bundle Adjustment	0.47±11.28	0.53±3.08	-0.68±104.83	0.98±105.48
26	VI	3	Bundle Adjustment	2.68±4.19	-3.29±5.17	-8.43±14.09	9.44±15.58
27	VI	4	Bundle Adjustment	0.09±0.40	0.63±1.58	-0.27±0.72	0.69±1.78
28	VI	5	Bundle Adjustment	-0.07±0.55	-0.07±0.68	-0.15±0.89	0.18±1.25
29	VI	8	Bundle Adjustment	0.28±0.50	-0.15±0.34	-1.03±0.69	1.08±0.92
30	VI	9	Bundle Adjustment	-0.12±0.33	-0.03±0.37	-0.44±0.49	0.46±0.70

Table 6. Error Computed at Checkpoints by Varying the Number of Control Points for Scenario VII (Projective).

Experiment #	Scenario	Number of Control Points	Estimation	Errors at checkpoints (Mean ± Std), meters			
				X	Y	Z	Spatial Error
31	VII	1	Bundle Adjustment	-	-	-	-
32	VII	2	Bundle Adjustment	-	-	-	-
33	VII	3	Bundle Adjustment	0.04±9.44	0.07±14.76	0.02±0.91	0.08±17.54
34	VII	4	Bundle Adjustment	0.51±0.43	-0.09±0.54	-0.44±0.61	0.68±0.92
35	VII	5	Bundle Adjustment	0.02±0.31	-0.10±0.57	-0.01±0.54	0.10±0.84
36	VII	8	Bundle Adjustment	0.33±0.48	0.11±0.33	-0.64±0.55	0.73±0.80
37	VII	9	Bundle Adjustment	-0.01±0.32	0.07±0.38	-0.32±0.55	0.33±0.74

Table 7. Error Computed at Checkpoints by Varying the Number of Control Points for Scenario VIII (DLT).

Experiment #	Scenario	Number of Control Points	Estimation	Errors at checkpoints (Mean ± Std), meters			
				X	Y	Z	Spatial Error
38	VIII	1	Bundle Adjustment	-	-	-	-
39	VIII	2	Bundle Adjustment	-	-	-	-
40	VIII	3	Bundle Adjustment	-	-	-	-
41	VIII	4	Bundle Adjustment	26.43±34.96	-8.51±12.69	0.38±1.72	27.77±37.23
42	VIII	5	Bundle Adjustment	1.99±8.83	3.44±7.86	0.06±1.12	3.97±11.87
43	VIII	8	Bundle Adjustment	0.34±0.43	-0.25±0.36	-1.00±0.73	1.09±0.92
44	VIII	9	Bundle Adjustment	-0.04±0.30	0.07±0.29	-0.28±0.55	0.29±0.69

CONCLUSIONS AND RECOMMENDATIONS

In this paper, we were attempting to increase the geometric accuracy of satellite imagery's rational polynomial coefficients. First and foremost we realized that original coefficients contain systematic errors which was evident from comparing the coordinates of control points with those derived from original RPC by means of forward intersection. A first degree polynomial correction to the rational polynomial coefficients was introduced and a photogrammetric triangulation using tie and control points was developed in order to estimate the corrections. Many models were analyzed, among which are shift, standard Affine, 2D Affine, projective transformation, DLT. It was clearly seen from the experiments that one of the most important correction is bi-directional shift. All of the tested models performed well with the existence of many control points, although models with larger number of parameters (such as DLT) slightly outperformed other model. As the number of control points decreases, most of the models (with the exception of DLT) performed similarly showing the need for at least five control points in order to archive sub-pixel accuracy.

Future work includes performing more tests to highlight the best model(s) for correcting rational polynomial coefficients. In addition, we will be attempting to investigate the quality of the control points and to improve image coordinate measurements by obtaining imagery with larger dynamic range (current imagery were obtained in 8 bits

which imposed some challenges to point identification). Furthermore, future research will also target reducing the number of control points by using different object space constraints.

REFERENCES

Abdel-Aziz, Y., and H. Karara, 1971. Direct linear transformation from comparator coordinates into object space coordinates in close-range photogrammetry, *Proceedings of ASP/UI Symposium on Close Range Photogrammetry*, 26-29 January, University of Illinois at Urbana Champaign, Urbana, Illinois, pp. 1-18.

Morgan, M., K. Kim, S. Jeong, and A. Habib, 2006. Epipolar resampling of space-borne linear array scanner scenes using parallel projection, *Photogrammetric Engineering & Remote Sensing*, 72(11):1255:1263.

Okamoto, A., S. Akamatsu, and H. Hasegawa, 1992. Orientation theory for satellite CCD line-scanner imagery of hilly terrains, *International Archives of Photogrammetry and Remote Sensing*, 02-14 August, Washington, D.C., Volume 29, Commission II, pp. 217-222.

Tao, V., and Y. Hu, 2001. A comprehensive study for rational function model for photogrammetric processing, *Photogrammetric Engineering & Remote Sensing*, 67(12):1347–1357.

Wang, Y., 1999. Automated triangulation of linear scanner imagery, *Joint Workshop of ISPRS WG I/1, I/3 and IV/4 on Sensors and Mapping from Space*, 27–30 September, Hanover, Germany, unpaginated CD-ROM.